CONTACTLESS INVESTIGATION OF THE P-TYPE DOPING CONCENTRATION LEVEL OF SINGLE MICROMETRIC SIZE GaAs CRYSTALS GROWN ON SILICON FOR MULTIJUNCTION SOLAR CELLS

Alexandre Jaffré[1], Jose Alvarez[1], Hung-Ling Chen[2], Hajer Makhloufi[2], Charles Renard[2],
Florent Loëte[1], Stéphane Collin[2], James Patrick Connolly[1], Jean-Paul Kleider[1], Denis Mencaraglia[1]
[1]GeePs, Group of Electrical Engineering Paris, CNRS, CentraleSupelec, Univ. Paris-Sud, Université Paris-Saclay,
Sorbonne Université, 3&11 rue Joliot-Curie, Plateau de Moulon, 91192 Gif-sur-Yvette CEDEX, France
[2]C2N, Centre de Nanosciences et de Nanotechnologies, CNRS, Univ. Paris-Sud, Université Paris-Saclay,
Avenue de la Vauve, 91120 Palaiseau, France

ABSTRACT: In previous work, we have demonstrated the perfect integration on silicon of micrometric GaAs crystals without any structural defects nor stress, using Epitaxal Lateral Overgrowth on Tunnel Oxide from nanoseeds (ELTOn). Then, it would be very interesting to integrate the crystals in a regular way to have a quasi-complete covering of the Si substrate, without coalescence of the GaAs microcrystals to maintain their very good electronic properties, avoiding then detrimental grain boundaries. The main focus of this work is to address the issue of the doping determination in a single micrometric size GaAs crystal which is a pre-requisite to develop the future design and technology of multijunction solar cells based on an array of non-coalescent GaAs crystals free of structural defects. In a previous work, local electrical characterizations by CP-AFM revealed a rather high non intentional p-type doping. To obtain a quantitative estimation of the doping level, we propose a contactless method based on the photoluminescence measurement of the evolution of the bandgap versus temperature and its modeling.
Keywords: Epitaxy, III-V Semiconductors, Doping, Photoluminescence, Multijunction Solar Cell, Silicon Solar Cell.

1 INTRODUCTION

For thirty years, researchers have been attempting to integrate III–V semiconductors, in particular, GaAs on silicon. However, three major intrinsic problems have to be overcome: the lattice parameter mismatch generating a high density of threading dislocations, the polar or non polar nature of GaAs or Si respectively, and the difference of thermal expansion coefficient, which is at the origin of cracks for thick GaAs layers [1]. Several approaches to these problems have been investigated to date, but until now, no one succeeded in achieving the defect-free and cost-effective integration of 2D continuous GaAs layers. One of these approaches, selective area epitaxy (SAE) of GaAs on patterned Si, has shown significant improvements, yielding mostly defect-free epitaxial layers. However, the relaxation process occurring at the GaAs/Si interface leads to a high density of misfit dislocations at levels, which are prohibitive for applications involving carrier transport through the interface area. We have recently demonstrated by a new method called ELTOn (for Epitaxial Lateral overgrowth on Tunnel Oxide from nano-seed) the defect- and strain-free heteropitaxy of micrometric GaAs crystal on Si, yielding an effective electrical contact of the epitaxial layer to the substrate [2].

An interesting consequence of this is that unlike many optoelectronic devices where continuous layers are desirable, the micrometric GaAs crystals form a textured surface which can be exploited to improve light management by reducing front surface reflection and contributing to light trapping. The GaAs array of non coalescent micro-crystals, free of structural defects, providing a quasi complete covering of the Si substrate, is therefore a promising route to III-V on Si mulltijunction solar cells.

Cost efficient multijunctions solar cells could be based on this approach if the doping of the GaAs microcrystals is fully controlled. However the doping level investigation on a single crystal is difficult by I(V) or C(V) measurements because in the first case the determination is too indirect and for the second, the determination is direct but the capacitance values will be too small to be evaluated.

It is then mandatory to develop a method sensitive enough to detect the doping level in one unique GaAs micrometric size crystal. The purpose of this work is to present such a contactless method based on the photoluminescence (PL) of a unique crystal which allows a precise measurement of the material bandgap energy. We have performed this measurement at different temperatures to investigate the bandgap evolution. Then modelling the bandgap dependence with temperature using published data and parametrized models of the literature, we could determine the doping density of a unique micrometric size GaAs crystal. This is not such an easy task both on an experimental or theoretical point of view. Indeed, experimentally even if the bandgap energy can be determined with a great accuracy from PL, the precise knowledge of the crystal lattice temperature is not always straightforward and can be somewhat different from the requested temperature. Some gradient can exist between the sample and the temperature probe, and also any significant sample heating by the laser excitation has to be avoided. Moreover, theoretically the semiconductors bandgap dependence with temperature is a complex physical problem for which up to now only semi-empirical relations have been proposed. Nevertheless a lot of work has already been performed on this topic and accurate parameter data sets are available, in particular for GaAs. To assess the validity of our method, we will first present its implementation on a nominally undoped GaAs bulk wafer (denominated here GaAs Ref sample), crosschecking the results with complementary experiments such as cathodo-luminescence for the bandgap determination, or a contactless Multi Frequency Eddy Current System (MFECS) that has been developed in GeePs to determine the GaAs Ref sample conductivity. Raman LO and TO peak positions were also measured with the same experimental conditions as for the PL measurements and compared to data of the literature for a strain free GaAs in order to have a better estimation of the lattice temperature of the samples under test.

2 EXPERIMENTAL SETUPS AND PROCEDURES

2.1 Micrometric size GaAs crystals growth

The micrometric size GaAs crystals were grown on silicon through a silica mask structured with nanoscaled openings (Fig. 1). The selective hetero-epitaxy ELTOn (for Epitaxial Lateral overgrowth on Tunnel Oxide from nano-seed) was realized by chemical beam epitaxy (CBE) at the growth temperature of 575 C using the gaseous precursors Trimethylgallium (TMGa) and Tertiarybutylarsine (TBAs). For more details of the growth procedure, and structural properties of our micrometric size GaAs crystals, the reader is referred to the previous studies [2 and our references therein].

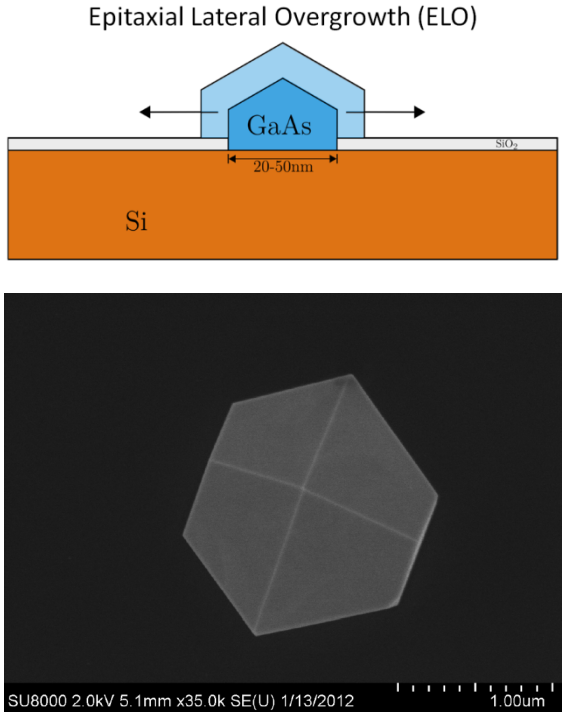

Figure 1: Top: Schematic view of Epitaxial Lateral overgrowth on Tunnel Oxide from nano-seed (ELTOn) through a silica mask structured with nanoscaled openings ; Bottom : Top SEM view of a micrometric size GaAs crystal grown on silicon using the ELTOn process.

2.2 µ-Photoluminescence/µ-Raman confocal microscope

µ-PL and µ-Raman measurements were performed on a WITec alpha-300R confocal microscope in a backscattering configuration. Samples were under vacuum at 10^{-3} mbar in a MMR cryostat and probed at a requested temperature imposed by the temperature controller from 100K to 450K, each 50K. Samples were excited at 532nm through an Olympus 20x long working distance objective, with 6.5mW laser power (82µW/µm²). This injection power is high but we verified that it does not affect the PL maximum peak position nor make the Raman peak shift. We choose this power to have enough Raman signal and to be able to compare PL and Raman in the same injection conditions. Raman scattered light is guided through a 50µm (pinhole) optical fiber to an UHTS300 spectrometer using a 1800 grooves/mm diffraction grating and a CCD silicon camera. For µ-PL analysis, we use a 200µm core diameter fiber, a Princeton SP-2300 spectrometer with a 150grooves/mm grating and an InGaAs CCD camera. Both cameras are cooled down to -70°C via 3-stages Peltier cooler.

Luminescence data are corrected by removing the spectral transfer function of the microscope. To achieve this we use an Ocean Optics HL-2000-CAL halogen calibration lamp. We place it as a point source under the microscope objective. Knowing the spectral irradiance of the lamp and measuring its spectra through the whole optical path (from the objective to the CCD camera), we are able to correct the luminescence data. The bandgap value of the sample is extracted for each temperature by evaluating the energy position of the maximum of the luminescence spectra.

Raman peak position and Full Width at Half Maximum (FWHM) are calculated by a Voigt function fit for each temperature step. Raman LO and TO peak positions for a strain free GaAs (ω(LO)=297.6cm^{-1} at 0K) are represented as a function of the requested temperature (not shown here) with an empirical model described in [3]. We compare our experimental data to this model and extract the local lattice temperature (denominated here Raman extracted temperature, T Raman extracted) by matching our Raman peak position values to the ones of the empirical model.

For PL and Raman measurements at each temperature step, we proceed as follows : we first reach 100K, then heat up the sample to 450K by taking spectra each 50K. For each step we wait five minutes before recording a spectrum to let the sample thermalize. We make two heat-up cycles with the same timing to be accurate, the first to collect PL, the second to record Raman scattering.

2.3 Nano-Cathodoluminescence

The nano-CL setup from Attolight brand is located at C2N. Cathodo-luminescence principle is based on the emission of light of a solid material which is excited with an electron beam. This tool has a spatial resolution down to 10nm. Samples were kept under vaccum in a He cryostat. CL measurements were performed at different temperature stages from 25K to 300K. The electron beam was accelerated at 6keV in order to have the same order of penetration depth in GaAs (~80nm) as for the 532nm PL excitation laser. Backscattered luminescence photons are injected in a spectrometer via a parabolic mirror. Spectral data were diffracted with a 150 grooves/mm grating and analyzed on a 3-stages Peltier cooled Silicon EMCCD camera. The Cathodo-luminescence data are also corrected with the spectral transfer function of the setup.

2.4 Conductance measurements

Conductance measurements have been achieved on our nominally undoped GaAs Ref sample in order to extract its conductivity and have an estimation of the doping concentration due to active residual impurities using a Multi Frequency Eddy Current System (MFECS) that has been developed in GeePs [4]. This patented contactless technique is based on eddy currents. The eddy current probe, constituted of a coil connected to a transmission line, interacts with the semiconductor wafer under inspection. The coil induces eddy currents in the semiconductor wafer that in return involve the creation of an induced magnetic field and a modification of the total magnetic field inside and in the vicinity of the wafer. The

coil impedance is measured by reflectometry using a broadband multicarrier test signal, i.e. containing multiple frequencies. An analytical electromagnetic model of the coil-wafer interaction is then used to estimate the conductivity of the wafer [5, 6].

3 MODELLING METHOD

For many years, the Varshni's semi-empirical relation has been used to describe semiconductors bandgap dependence with temperature [7]. However the inadequate analytical structure of Varshni's formula was explained by Pässler in 1999 who proposed an analytical four-parameters expression capable of providing better numerical fittings and estimations of physical parameters [8]. Pässler refined further this work in 2003 [9] but considering our investigated temperature range, for the present purpose it is sufficient to use the previously proposed analytical four-parameters expression written as

$$E(T) = E(0) - \frac{\alpha\theta_p}{2}\left[\sqrt[p]{1+\left(\frac{2T}{\theta_p}\right)^p} - 1\right], \qquad (1)$$

with, in the GaAs case, the following values of the four parameters :
E(0) = 1.519 eV, p = 2.44, α = 0.472 meV/K, θ_p = 230 K and T being the sample lattice temperature.
This four-parameter Pässler's data set has been determined by fitting the high precision PL data of Grilli et al. [10] measured on a high-quality nominally undoped GaAs sample grown by molecular beam epitaxy.
For heavily p-type doped samples, we take into account the band gap narrowing (BGN) substracting to the right hand-side of Eq. (1) the expression of ΔE_{BGN} given by

$$\Delta E_{BGN} = AP^{\frac{1}{3}} + BP^{\frac{1}{4}} + CP^{\frac{1}{2}}, \qquad (2)$$

where P is the active dopant concentration, A, B, and C having the following constant values:
A = 9.83x10^{-9} eV/cm, B = 3.90x10^{-7}eV/cm$^{3/4}$, C = 3.90x10^{-12} eV/cm$^{3/2}$ for p-type GaAs if ΔE_{BGN} is expressed in eV and P in cm^{-3} [11].
We will show that a least-square fit of our experimental data, without any change in the parameters of Eqs. (1) and (2) allowed us to have a good estimation of the active dopant density. The quality of the fits will be compared using either the requested temperature or the Raman extracted one defined in section 2.2.

4 RESULTS AND DISCUSSION

4.1 Validation of the accurate bandgap extraction

To check the accuracy of our experiments we first worked on a GaAs reference bulk and have done several cross-checks on it. The first step was to compare PL and CL spectra at 300K in equivalent experimental conditions (6keV electron acceleration for the CL so that the penetration depth is around 80nm in GaAs, equivalent to the 532nm PL Laser penetration depth). Figure 2 shows normalized PL and CL spectra in semi-log scale for our GaAs reference wafer. The curves are well superimposed around the bandgap value. On the PL spectrum we notice some noise at higher energies. This is due to the fact that PL detector is an InGaAs CCD camera, so the noise is important in this low CCD sensitivity region. We also notice that the slope of the high energy part is not constant on the PL spectra compared to the CL ones. This could be the consequence of hot carriers effect during the PL experiment.

In the low energy region, the noise is higher on the CL results. The reason is the same than previously but this time, it is correlated to low sensitivity of the Si CCD camera in this energy range. This comparison shows that the spectral acquisition is well calibrated. We also performed this study on the crystal and the curve behaviors are the same. From this point we extract the bandgap value of our sample by evaluating the energy position of the maximum of the luminescence spectra. At 300K, we extract a bandgap value of 1.422eV for the GaAs reference bulk which is in agreement with the literature [12].

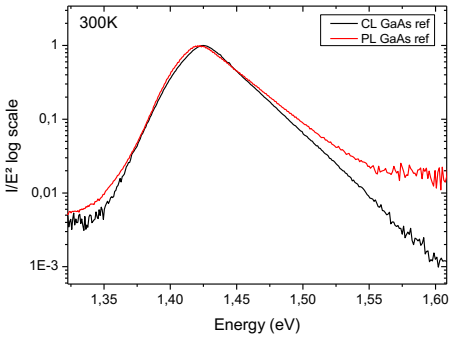

Figure 2: PL and CL spectral comparison at 300K on the reference bulk

4.2 Assessment of the undoped GaAs bulk reference quality

We performed Raman spectroscopy measurements at 300K of our undoped GaAs (100) reference bulk (Fig. 3). TO and LO modes position and FWHM are consistent with values given in the literature for an undoped GaAs bulk [13].

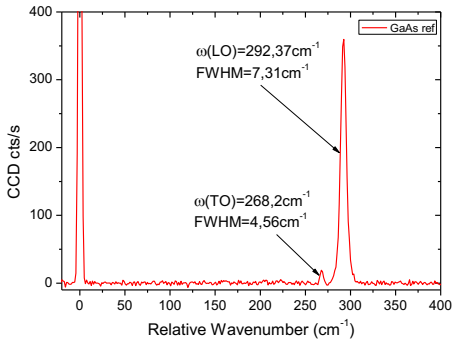

Figure 3: Raman spectrum of the undoped GaAs (100) reference bulk at 300K.

Our Multi Frequency Eddy Current System (MFECS) setup was used to derive the conductivity at room temperature of our 444 µm thick undoped GaAs reference sample. The MFECS data and its fit are shown in Fig. 4. The normalized coil impedance variation δZ /X0 due to the presence of the sample can be modeled as a function of the layer properties (conductivity, thickness) [6]. Knowing the thickness of the wafer, its conductivity was derived to be equal to 5.Ω^{-1}cm^{-1}, probably due to residual electrically active impurities. Taking into account the mobility dependence versus doping content, such a conductivity can be attributed either to a n-type doping around 5.10^{15} cm^{-3}, or to a p-

type one around 2.10^{17} cm^{-3}. However such a rather high p-type doping content would have led to a bandgap narrowing effect easily detectable with our PL measurement. This is not the case as we will see later in this section (refer to Fig. 5). Then the only hypothesis left is a light n-type doping density around 5.10^{15} cm^{-3}. This shows that our unintentionally doped GaAs Ref behaves as a lightly n-type doped sample due to a low residual doping level that does not affect significantly the temperature dependence of the bangap as we will see in the next paragraph.

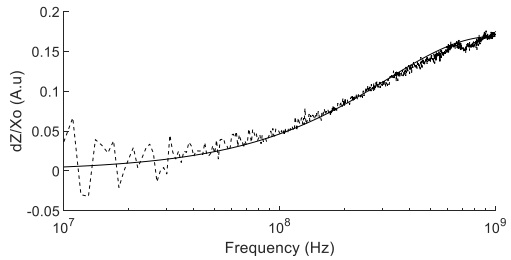

Figure 4: Comparison of the experimental (dashed line) and fitted (full line) normalized impedance variation of the coil in presence of the GaAs sample, as a function of frequency

Figure 5 shows the temperature dependence of the bandgap of our GaAs reference wafer derived from PL measurements (symbols) compared to the Pässler's analytical four-parameters set of data (full line) calculated with Eq. 1.

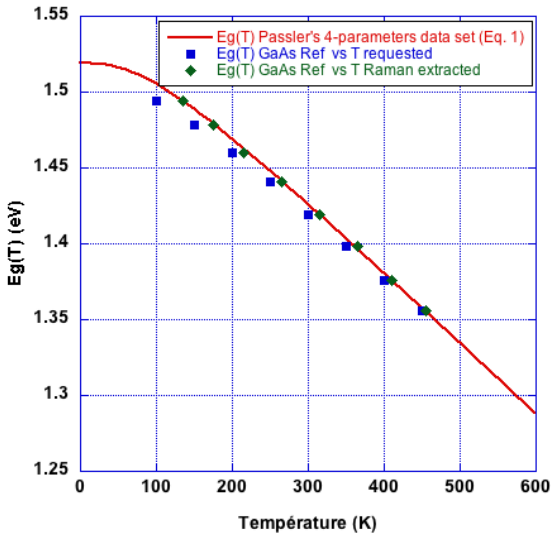

Figure 5: Temperature dependence of the bandgap of our GaAs reference wafer derived from PL measurements (symbols) compared to the Pässler's analytical four-parameters set of data (full line) calculated with Eq. 1.

We can note that using the Raman extracted temperature to deduce the lattice temperature of the sample under test, a perfect agreement is obtained between the bandgap temperature evolution of our GaAs Ref sample and the one modeled with Pässler's Eq.1 for a high quality undoped GaAs sample. This comparison also attests for the very good quality of our GaAs Ref sample and permits to validate the better estimation of the lattice temperature when using the Raman extracted temperature instead of the requested temperature.

4.3 Extraction of the doping density on a single GaAs crystal grown on silicon

Figures 6 and Figure 7 show the temperature dependence of the bandgap of a GaAs crystal derived from PL measurements, when the lattice temperature has been taken equal to the requested one or to the Raman extracted one, respectively.

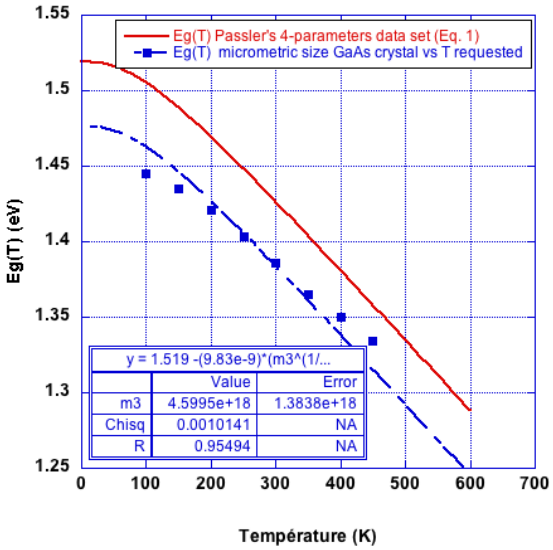

Figure 6: Temperature dependence of the bandgap of a micrometric size GaAs crystal grown on Si derived from PL measurements (symbols); curve fit (dashed line) using Pässler's Eq.1 (full line) corrected for the bandgap narrowing (Eq.2). The temperature in this figure corresponds to the requested one.

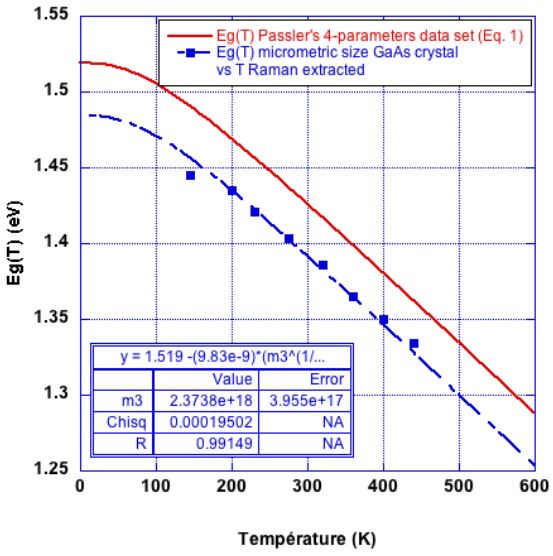

Figure 7: Temperature dependence of the bandgap of a micrometric size GaAs crystal grown on Si derived from PL measurements (symbols); curve fit (dashed line) using Pässler's Eq.1 (full line) corrected for the bandgap narrowing (Eq.2). The temperature in this figure corresponds to the Raman extracted one.

In both figures, the full line represents the Pässler's analytical four-parameters set of data calculated with

Eq.1 for a nominally undoped GaAs sample and the dashed line corresponds to the fit using Pässler's Eq.1 corrected for the bandgap narrowing (Eq.2). The quantitative result of the fit with the doping concentration as the only unknown parameter is given in the inserted tables of both figures, where m3 (representing P of Eq. 2) is the fitted variable. We can note the better quality of the fit in Fig. 7 when the lattice temperature has been taken equal to the Raman extracted one, leading to a p-type doping density comprised between $2.0x10^{18}$ cm^{-3} and $2.8x10^{18}$ cm^{-3}.

Such a rather high doping content has been attributed to carbon incoporation during the Epitaxal Lateral Overgrowth on Tunnel Oxide from nanoseeds (ELTOn) process using TriMethyl-Gallium (TMGa) and TertiaryButyl-Arsine (TBAs) as gas precursors [14]. This high carbon doping has been observed in the literature, and one of the proposed solutions to control the carbon incorporation is to adjust the concentration by the simultaneous use of TEGa (TriEthyl-Gallium) and TMGa together with TBAs. Using TEGa and TMGa in variable proportions is expected to allow a good control of the level of doping over a range from 10^{14} cm-3 to 10^{20} cm-3 [15]. This will be investigated in the future with the method presented in this paper which we have shown able to determine the doping content in a single micrometric size GaAs crystal.

5 SUMMARY

In this paper, contactless methods (PL, CL, Raman thermography) were investigated to determine the doping level on a single micrometric size GaAs crystal from the bandgap evolution with temperature. We have seen that the precise knowledge of the lattice temperature is a critical point to derive a good estimation of the doping level. Raman Stokes shift analysis versus temperature has been used to extract a more accurate determination of the lattice temperature of the sample under test than the requested one. The refined method presented here has permitted to have a better estimation of the p-type doping level due to carbon incorporation already observed in our previous works and attributed to an incomplete decomposition of the TMGa precursor gas used in our Epitaxal Lateral Overgrowth on Tunnel Oxide from nanoseeds (ELTOn) process. This characterization technique will be useful in the future to investigate the doping control of the GaAs crystals using a mixture of TMGa and TEGa as gas precursors during the growth process. If such a doping control during our ELTOn growth process can be achieved for both n- and p-type, the GaAs array of non coalescent micrometric size crystals, free of structural defects, providing a quasi complete covering of the Si substrate, could be a very promising route for cost efficient III-V on Si mulltijunction solar cells.

Acknowledgments

This work was supported by the ANR (project MULTISOLSI No. 2011 PRGE 00901). The authors also thank the Centrale de Technologie Universitaire MINERVE and RENATECH for technological backup.

References

[1] S. F. Fang, K. Adomi, S. Iyer, H. Morko, H. Zabel, C. Choi, and N. Otsuka, J. Appl. Phys. 68, R31 (1990)

[2] C. Renard, T. Molière, N. Cherkashin, J. Alvarez, L. Vincent, A. Jaffré, G. Hallais, J.P. Connolly, D. Mencaraglia, and D. Bouchier, Sci. Rep. 6, 25328 (2016)

[3] A. M. Ardila, O. Martínez, M. Avella, J. Jiménez, B. Gérard, J. Napierala, and E. Gil-Lafon, J. Appl. Phys. 91, 5045 (2002)

[4] D. Mencaraglia, Y. Le Bihan, F. Loëte, Contactless measurement of the conductivity of semiconductors, Patent FR 15 53392, 16/04/2015; WO2016/166449A1

[5] F. Loete, Y. Le Bihan and D. Mencaraglia, IEEE sensors journal, vol. 16, no. 11, pp.4151-4152, 2016

[6] C. V. Dodd and W. E. Deeds, J. Appl. Phys. 39, 2829 (1968)

[7] Y. P. Varshni, Physica 34, 149 (1967)

[8] R. Pässler, Phys. Stat. Sol. (b) 216, 975 (1999)

[9] R. Pässler, Phys. Stat. Sol. (b) 236, No. 3, 710 (2003)

[10] E. Grilli, M. Guzzi, R. Zamboni, and L. Pavesi, Phys. Rev. B 45, 1638 (1992)

[11] S. C. Jain, J. M. McGregor, and D. J. Roulston, J. Appl. Phys. 68, 3747 (1990)

[12] O. Madelung et al., Group III Condensed Matter 41A1b - Group IV Elements, IV-IV and III-V Compounds; p. 1174

[13] O. Madelung et al., Group III Condensed Matter 41A1b - Group IV Elements, IV-IV and III-V Compounds; p. 1470

[14] T. Moliere, A. Jaffre, J. Alvarez, D. Mencaraglia, J.P. Connolly, L. Vincent, G. Hallais, D. Mangelinck, M. Descoins, D. Bouchier and C. Renard, J. Appl. Phys. 121, 035704 (2017)

[15] H. Lüth, *Solid Surfaces, Interfaces and Thin Films*, Springer Science & Business Media, 2 sept 2010, p. 166